X-ray absorption spectroscopic study on A_2FeReO_6 double perovskites

2005 J. Phys.: Condens. Matter 17 4963

(http://iopscience.iop.org/0953-8984/17/33/002)

INSTITUTE OF PHYSICS PUBLISHING JOURNAL OF PHYSICS: CONDENSED MATTER

J. Phys.: Condens. Matter **17** (2005) 4963–4976 doi:10.1088/0953-8984/17/33/002

X-ray absorption spectroscopic study on A_2FeReO_6 double perovskites

J Herrero-Martín, G Subías, J Blasco[1], J García and M C Sánchez

Instituto de Ciencia de Materiales de Aragón, CSIC-Universidad de Zaragoza, Departamento de Física de la Materia Condensada, C/Pedro Cerbuna 12, 50009 Zaragoza, Spain

E-mail: jbc@unizar.es

Received 26 May 2005, in final form 23 June 2005
Published 5 August 2005
Online at stacks.iop.org/JPhysCM/17/4963

Abstract

The electronic and geometrical local structures of Re-based double perovskites, A_2FeReO_6 (A = Ba, Sr, Ca), have been probed by using x-ray absorption spectroscopy at the Fe K- and Re $L_{1,2,3}$-edges. The measurements have shown a significant sensitivity of the Fe K- and Re L_1-edges to the Fe and Re valences, respectively. EXAFS and XANES spectra are consistent with the presence of nominal Fe^{3+} and Re^{5+} except for the Ba-based compounds. Ba strongly affects the charge distribution on the Fe–O–Re sublattice, leading to mixed valence $Fe^{3-\delta}$ ions. We have explained our results in the frame of recent band models. In this way, pre-peak features at the Re L_1-edge can be used as an indicator of the degree of pd hybridization existing in these systems.

(Some figures in this article are in colour only in the electronic version)

1. Introduction

A renewed interest has been focused in the last years on the $A_2BB'O_6$ (A being alkaline earth and B/B′ being transition metal) compounds with perovskite structure. The reason is the outstanding magnetic and electronic properties they exhibit as a consequence of the strong interplay between structure, charge and spin ordering [1]. This fact, combined with the discovery of their tunnelling type magnetoresistance at room temperature [2], makes them very interesting materials to be used in spintronic devices, among others. In particular, the series with B and B′ being Fe and Re ions is very promising due to their high values of T_C [3, 4], far above room temperature. The A_2FeReO_6 compounds are ferrimagnetic at room temperature but the physical properties strongly depend on the A type. Whereas Sr- and Ba-based compounds are metallic in the ferrimagnetic state [4–6], the temperature dependence of the Ca-compound conductivity is thermally activated [4–10]. The latter compound also shows

[1] Author to whom any correspondence should be addressed.

a phase transition at ∼150 K together with an increase in its resistivity that was the object of controversy. Several authors claimed a mesoscopic phase separation at low temperature [8, 9] with up to three monoclinic phases coexisting below 150 K. Other authors instead suggested the existence of a spin reorientation coupled to a slight change in the local environment of the Fe atom at that temperature [10].

The crystallographic structure of A_2FeReO_6 compounds also depends on the A atom size. Thus, the smaller the A cation is, the lower the symmetry of the unit cell. While Ba_2FeReO_6 and $BaSrFeReO_6$ crystallize in a cubic cell, Sr_2FeReO_6 has a tetragonal structure and the Ca-based compounds are monoclinic [5]. A similar kind of dependence was also found in the related A_2FeMoO_6 series [11] but all the samples have metallic behaviour in this case. Another difference between both series concerns the magnetic properties. Re-based double perovskites are magnetically hard [4] and Mo compounds are magnetically much softer [2]. Moreover, the highest T_c (∼410 K) in the Mo-based series corresponds to Sr_2FeMoO_6 [11, 12] and this fact was understood in terms of the superexchange interaction J. In this way, J increases as the unit cell decreases for the Sr and Ba compounds with straight Fe–O–Mo bond angles. The Ca compound instead, with Fe–O–Mo angles smaller than 180°, has a lower J and T_C. This mechanism does not seem to operate in the Re-based compounds, where the T_C continuously increases with decreasing A size independently of the Fe–O–Re bond angle [5, 6]. The opposite occurs with the transport properties: the Ca_2FeReO_6 is an insulator while Ca_2FeMoO_6 is metallic. In this case, the small Fe–O–Mo(Re) bond angle only seems to affect the bandwidth of the former compound.

In order to gain insight into the properties of these double perovskites, a deep knowledge of the electronic configuration is required. The classical description for these compounds lies in the following valence degeneracy of the electronic states: $Fe^{3+} + Mo(Re)^{5+} \leftrightarrow Fe^{2+} + Mo(Re)^{6+}$. Several spectroscopic studies have been devoted to finding the better description for this system, giving rise to controversies. In this way, Mössbauer experiments on Mo-based compounds have been interpreted in terms of the presence of either Fe^{3+} [13] or an Fe^{3+}/Fe^{2+} mixture [14]. Similarly, x-ray absorption spectroscopy (XAS and XMCD) measurements on Sr_2FeMoO_6 at the Fe L-edge also concluded the presence of Fe^{3+} [15] or an intermediate valence Fe^{3+}/Fe^{2+} [16–18]. Fewer works have been devoted to studying the electronic state of Mo(Re) atoms. In related samples (Cr based) and making use of the Mo L_3-edge XAS, some authors have identified Mo^{6+} and $Mo^{5.5+}$, suggesting a relationship between Mo valence and oxygen content in the double perovskite [19]. Recently, photoemission spectroscopy (PES) has been used to characterize Sr_2FeMoO_6 doped with La [20]. These authors found two distinguishable electronic states, 66% of Mo^{6+} and 34% of Mo^{5+}, in the 3d-Mo spectra, suggesting a $3d^{6-\delta}$ ($\delta \sim 0.33$) state for Fe atoms (and thus, close to +2).

Previously, we also studied the A_2FeMoO_6 series by means of the XAS technique [21]. We measured x-ray absorption near edge structure (XANES) and extended x-ray absorption fine structure (EXAFS) spectra at the Fe and Mo K-edges. We found that the Fe K-edge spectra depend on the A-type atom while the Mo K-edge ones are almost equal for all the samples, putting forward the difficulty to differentiate between Mo^{5+} and Mo^{6+}. Our work did not support the presence of integer ionic states for all samples in this series and we proposed, in accordance with Szotek *et al* [22], an Fe^{3+}/Mo^{6+} ground state coupled antiferromagnetically to an itinerant electron. The electron projection on either Fe^{3+} or Mo^{6+} would give rise to the observed intermediate valence [16–18, 20].

To the best of our knowledge, there has not been a systematic XAS study on the whole A_2FeReO_6 series comparing the role of the A atom. We here report XANES and EXAFS measurements at Fe K- and Re L-edges in order to characterize electronic and structural changes along the series.

2. Experimental details

The samples were prepared by solid state reaction by mixing stoichiometric amounts of A_2CO_3 (A_2: Ba, Sr, Ca), Fe_2O_3, ReO_3 and Re as described elsewhere [6]. They were pressed into pellets and heated at 1000 °C for 3 h in a pure Ar atmosphere. We have synthesized $(AA')_2FeReO_6$ compositions where $(AA')_2 = Ba_2$, BaSr, Sr_2, SrCa, $Ca_{3/2}Sr_{1/2}$ and Ca_2. Hereafter we will denote the samples indicating the A atom. X-ray diffraction measurements revealed single phase for all compositions. The full characterization is also reported elsewhere [6].

X-ray absorption spectra were recorded at the BM29 beamline of the ESRF in Grenoble, France [23]. The measurements were performed in transmission mode on powder samples. The incident and transmitted beams were detected by means of ionization chambers. The storage ring operating conditions were 6 GeV electron energy and ∼190 mA electron current. The beam was monochromatized by a fixed-exit Si(311) double crystal at both the Fe K- and the Re L_i-edges. Harmonic rejection was achieved by 50% detuning of the monochromator from the parallel alignment. The energy resolution $\delta E/E$ was estimated to be about 4×10^{-5} and 1×10^{-4} at the Fe K- and Re L_i-edges, respectively. XANES spectra were taken for the Fe K- and Re $L_{1,2,3}$-edges while EXAFS spectra were measured at the Fe K- and Re L_3-edges. Both kinds of spectra were collected at 40 K and at room temperature (∼295 K). An Fe foil and a pellet of metallic Re were simultaneously measured for energy calibration. The XANES spectra were normalized to the high energy part of the spectrum (∼100 eV beyond the edge) after background subtraction. The EXAFS structural analysis was mainly restricted to the first coordination shell by means of the FEFF 8.10 code and FEFFfit package [24]. The fits were carried out in the R-space. We have also measured $LaFeO_3$, FeO, ReO_2 and ReO_3 as reference compounds.

3. Results

3.1. Fe K-edge XANES

Figure 1(a) shows the Fe K-edge XANES spectra at 40 K for the whole series. These spectra are compared to Fe^{2+} (FeO) and Fe^{3+} ($LaFeO_3$) references. The latter also crystallizes in a perovskite unit cell. The XANES spectra of A_2FeReO_6 strongly resemble those of A_2FeMoO_6 samples [21], suggesting a similar evolution for both series.

The XANES spectra of A_2FeReO_6 samples are quite structured, showing well defined features. The main traits of these spectra are a strong resonance at the threshold (denoted as W in figure 1(a)), some pre-peak structures at ∼15 eV below W (denoted as P) and shoulders at intermediate energies (S). W and S are ascribed to dipolar $1s \rightarrow np$ transitions whose shape and intensity are related to local geometrical characteristics such as the scattering power of the A atom. In this way, Ba_2 and Ca-based samples show a strong W resonance while the weakest one corresponds to the Sr_2 compound. Feature P, also present in the $LaFeO_3$ spectrum, appears at ∼7114 eV for all A_2FeReO_6 samples. This resonance is ascribed to $1s \rightarrow 3d$ transitions, either quadrupole allowed or dipole forbidden for an octahedral environment. The latter becomes permitted due to a strong mixing between O 2p and Fe 3d states. The P intensity does not change along the A_2FeReO_6 series as occurs in the related A_2FeMoO_6 samples [21]. Moreover, S also appeared in the Mo series near the edge position, though it showed higher intensity in Mo samples. A comparison between both series reveals that the Fe K-edge energies of A-related compounds in each series are almost identical no matter whether the substituted transition metal B′ is Mo or Re, depending only on the divalent cation A.

The room temperature A_2FeReO_6 XANES spectra are almost identical to the ones reported in figure 1(a). This is even true for the Ca-based samples showing an electronic transition at

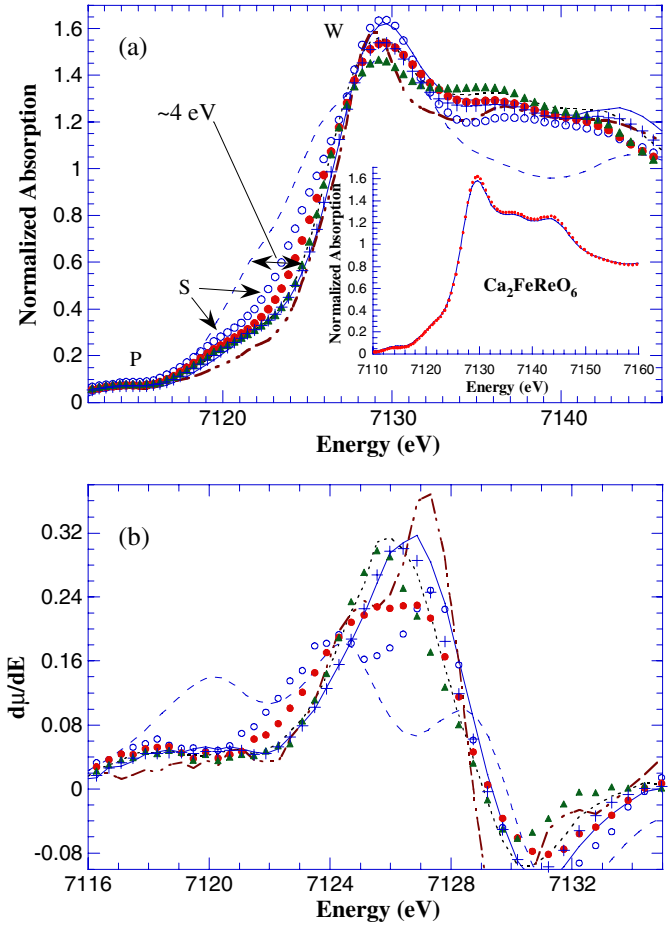

Figure 1. (a) XANES spectra of the A_2FeReO_6 and reference samples at the Fe K edge at 40 K, A_2 being Ba_2 (open circles), BaSr (filled circles), Sr_2 (triangles), CaSr (dotted line), $Ca_{3/2}Sr_{1/2}$(+), Ca_2 (solid line), $LaFeO_3$ (chain curve) and FeO (dashed line). Inset: comparison of the XANES spectra at 40 K (points) and room temperature (line) for Ca_2FeReO_6. The letters W, S and P denote white line, shoulders and pre-edge features, respectively. (b) Differentiated spectra close to the threshold. The symbols have the same meaning as in (a).

∼150 K, as can be seen in the inset of figure 1(a). This result reveals that no significant changes occur in the geometrical and electronic structure around the Fe atoms in the whole temperature range up to room temperature.

The main difference among the samples concerns the edge position. Commonly, the edge value is taken from the first inflection point. As the edge is very structured for the references, we have used the centroid resulting in 7122.0 and 7126.0 eV for FeO and $LaFeO_3$, respectively. Then, the edge shift between our references is close to 4 eV, a value in agreement with the observed chemical shift between Fe^{2+} and Fe^{3+} compounds [25]. Overall, the threshold of A_2FeReO_6 samples lies closer to the Fe^{3+} reference spectrum, especially for Sr- and Ca-based compounds. The differentiated spectra, shown in figure 1(b), reveal a broad maximum for Sr_2, CaSr, $Ca_{3/2}Sr_{1/2}$ and Ca_2 samples. The Ba_2 and $LaFeO_3$ instead have two peaks, whereas the BaSr compound displays an intermediate behaviour. Similar curves were reported for the Mo series in [21].

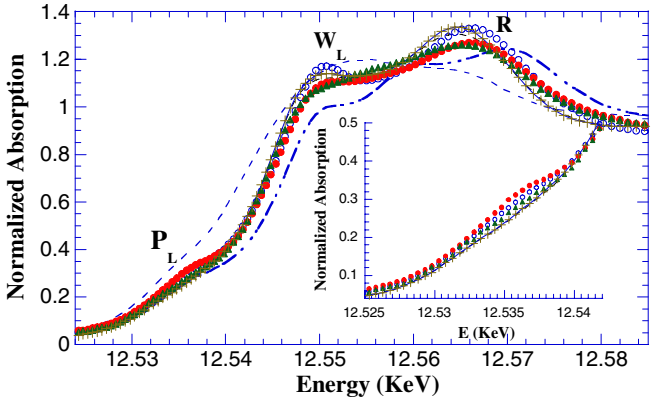

Figure 2. XANES spectra of the A_2FeReO_6 and reference samples at the Re L_1 edge at room temperature, A_2 being Ba_2 (open circles), BaSr (filled circles), Sr_2 (triangles), CaSr (dotted line), $Ca_{3/2}Sr_{1/2}$(+) and Ca_2 (solid line). ReO_2 (dashed line) and ReO_3 (chain curve) serve as reference. Some features are marked as P_L, W_L and R that stand for pre-edge, white line and resonance, respectively. Inset: detail of the pre-edge features for A_2FeReO_6 compounds.

In order to perform the comparisons we have used the centroid of the derivative curve as the first inflection point. In this way, the calculated edge values are 7125.0, 7125.7 and 7126.0 eV for Ba_2, BaSr and the rest of the A_2FeReO_6 samples, respectively. Therefore, the edge position for the latter samples is consistent with the presence of trivalent Fe, whereas a mixed valent Fe (∼+2.75) can be deduced for Ba_2, following a linear approach between edge shift and oxidation state as occurs in related compounds [26]. The Fe in BaSr shows an intermediate behaviour but its oxidation state would be close to +3. However, the valence assignation from XANES spectra, even for Ba_2, must be made with care and should be confirmed by EXAFS spectra in order to have a self-consistent analysis.

3.2. Re $L_{1,2,3}$-edge XANES

The XANES spectra at the Re L_1-edge for these samples are shown in figure 2. The reference spectra nicely agree with previously reported ones [27] whereas the A_2FeReO_6 spectra are composed by a strong resonance (R) at ∼15 eV above the white line (W_L) and a significant pre-edge (P_L) below the threshold at about 12 535 eV. This pre-edge is present for all the compounds and corresponds to 2s → 5d transitions that are dipole forbidden. Nevertheless, a strong overlap of Re 5d with O 2p orbitals results in a considerable transition probability [27]. Then, P_L reveals the degree of d–p orbital mixing. The inset of figure 2 shows in detail the P_L features for the A_2FeReO_6 samples. Clearly, the insulator samples (Ca_2 and $Ca_{3/2}Sr_{1/2}$) have the weakest P_L, supporting a close relationship between p–d mixing and metallic behaviour. The strong feature R is associated with multiple scattering paths contributing significantly to the absorption at low momentum k of the photoelectron. Finally, the white line is located around 12 551 eV for all A_2FeReO_6 samples.

The L_1-edge is mainly caused by 2s → np electronic transitions and roughly gives the same information as the K-edge because it measures the density of projected p-states. A first glance at figure 2 suggests an intermediate position of the edge for all A_2FeReO_6 samples. Accordingly, an intermediate valence close to 5+ is inferred. The edge energy position, taken as the inflection point or peak-centroid in the first derivative (figure 3), shifts from 12 542.2 eV in ReO_2 to 12 546.4 eV in ReO_3, giving rise to a chemical shift of 4.2 eV between Re^{4+} and

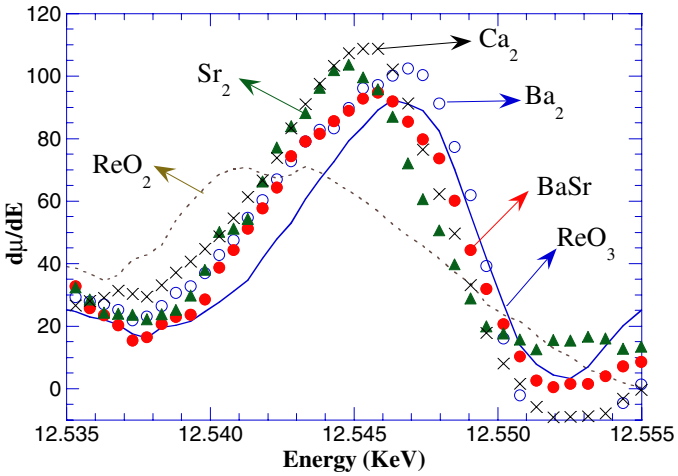

Figure 3. Differentiated XANES spectra (figure 2) for ReO_2, ReO_3 and A_2FeReO_6 samples. The name of the sample is indicated for each curve. For the sake of clarity, the data for CaSr and $Ca_{3/2}Sr_{1/2}$ are omitted but their curves are almost the same as that of Ca_2.

Re^{6+}. The edge for most of the A_2FeReO_6 samples lies at 12 545.0 eV, that can be taken as the edge position for Re^{5+}. The Ba_2 and BaSr samples also show broad derivative peaks, especially for the former, and their centroids are located at 12 545.5 eV. Therefore, a higher oxidation state cannot be discarded for the Re in these compounds, though it would be very close to +5. Moreover, this assignation would be in accordance with the results deduced from the Fe K-edge spectra (see figure 1), showing a correlation with the reduced Fe atoms in Ba-based compounds.

The XANES spectra at the Re L_2- and L_3-edges are shown for the whole series in figure 4. They are compared to two references, ReO_3 (Re^{6+}) and ReO_2 (Re^{4+}). The Re $L_{2,3}$-edge spectra are characterized by strong white lines as expected from the presence of empty 5d states [28, 29]. The Re L_3 spectra for A_2FeReO_6 samples have a high resemblance to each other and, in fact, all compounds have the same edge energy position (10 539.0 eV). The white line ($2p_{3/2} \rightarrow 5d$) reflects the presence of a splitting showing a continuous evolution from Ba to Ca; the latter clearly displays both peaks. The first maximum (P_1) appears at about 10 540.1 eV and a second stronger peak (P_2) is located 3.5 eV above in all the spectra. This splitting is characteristic of 4d- and 5d-metal compounds with an octahedral coordination [30, 31] and it has also been observed in related Re compounds [32]. The energy splitting is generally ascribed to the crystal field splitting of d orbitals into t_{2g} and e_g states [33] but it is noteworthy that such a splitting is related but not equal to the crystal field parameter, $10Dq$. This is due to the implied electronic transitions, from a d^n ground state to a p^5d^{n+1} final state [30].

The edge energies of the references are located at 10 538.2 and 10 539.4 eV for ReO_2 (Re^{4+}) and ReO_3 (Re^{6+}), respectively. The latter shows a white line of similar intensity to those observed in the samples of the series, while the former has a rather lower peak. No shoulder appears in any of the references, though a broad and asymmetric width of their peaks could indicate the presence of two overlapped components. The small displacement in the position of the Re L_3-edge between the Re^{4+} and Re^{6+} references points to a weak dependence of this edge on the oxidation state of the transition metal ion. Considering the spectral centroid, the Re L_3-edge centroid in our samples is situated in between both references, suggesting a formal valence close to +5 for the rhenium atoms in all of them. However, it is worth emphasizing the energy splitting again. Several authors have related such an energy splitting to the crystal

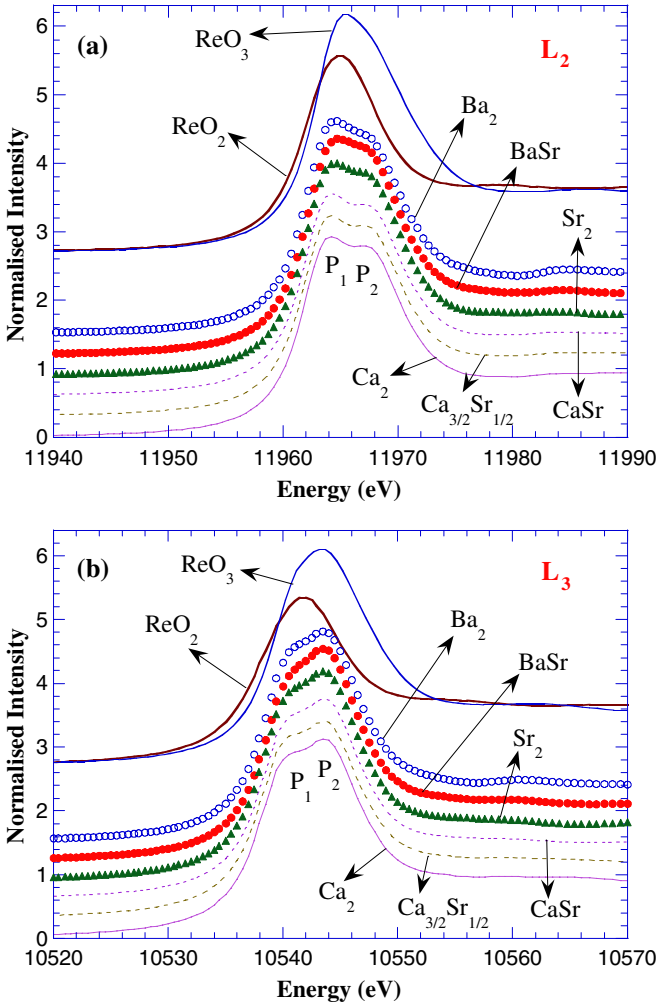

Figure 4. XANES spectra at the (a) Re L_2-edge and (b) Re L_3-edge for the A_2FeReO_6 samples. A_2 is given for each curve and the data were taken at room temperature. The reference compounds, ReO_2 and ReO_3, are also shown for the sake of comparison. Spectra are shifted in the vertical axis for the sake of clarity.

field splitting, $10Dq$. In this way, an increase of the atomic valence leads to an increase of both $10Dq$ and L_3-splitting as observed in other systems [34]. In our case, this approximation does not apply because the highest L_3-edge splitting is observed at intermediate valence. We think our splitting could also be related to the presence of two electronic states for Re atoms as observed in Mo-based double perovskites by means of other spectroscopic techniques [20]. In this way, similar L_3-edge splitting has also been observed in Mo double perovskites with a formal mixed valence for Mo atoms [32].

The Re L_2-edge XANES spectra for the same samples are collected in figure 4(a). This edge concerns $2p_{1/2} \rightarrow 5d$ transitions. We observe a similar energy splitting of the white line but the relation of amplitudes P_1/P_2 is inverted, making the Re L_2-spectrum a mirror image of that at the Re L_3-edge (figure 4(b)). This fact has also been observed in related systems [35]. This is a consequence of the different transition probability to the 5d orbital

final states depending on the initial state of the photoelectron [33]. Therefore, the main peak is now located at 11 964.3 eV and the second maximum is ∼3 eV above. As observed in the Re L_3-edge, the resonances are almost equal for all A_2FeReO_6 samples.

Finally, it is worth pointing out that no significant differences were found between Re L-edge spectra measurements at 40 K and at room temperature, indicating that minor changes occur in the local geometrical–electronic structure of the Re atom in this temperature range.

3.3. EXAFS spectra

The EXAFS spectra were measured at 40 K and at room temperature. The spectra turned out to be very alike for both temperatures except for the attenuation of oscillations as temperature increases. Therefore, the discussion in this section will be focused on the data at low temperature but the conclusions can be extended up to room temperature.

Figure 5 displays the Fe K-edge EXAFS spectra for all A_2FeReO_6 samples. The EXAFS oscillations extend up to $k \sim 14$ Å^{-1} with high signal-to-noise ratio. The spectra show a continuous evolution from the cubic Ba_2 to the monoclinic Ca_2. The monoclinic compounds have the least intense oscillations for higher shells due to the low structural symmetry. The Fourier transform (FT) of the k-weighted EXAFS spectra was calculated between 2.5 and 13.0 Å^{-1} using a Gaussian window and structural features are noticeable up to ∼6 Å as can also be seen in figure 5. FT curves exhibit a strong peak at around 1.5 Å due to the first coordination shell. This peak corresponds to the average Fe–O distances after phase-shift correction. At first glance, it seems that larger Fe–O distances are found for the Ba-based samples. Further peaks up to ∼4 Å arise from second coordination shells due to several single- (Fe–Re, Fe–A) and multiple- (Fe–O–O, Fe–O–Re) scattering paths. The monoclinic phases (Ca-based compounds) show a set of peaks with small intensity as expected from the large spread of interatomic distances due to the low structural symmetry. Stronger peaks are observed for samples with cubic symmetry (Ba-based compounds) but the highest intensity corresponds to the tetragonal Sr_2 sample with a strong peak centered at 3.2 Å. Similar results were obtained for the Mo-based double perovskites [21] whose spectral differences in FT curves mainly arise from the different scattering atoms (A-type) presented in the second shell.

The structural analysis was performed in the R space fitting mode using the FEFF 8.10 package [24]. The analysis was restricted to the first coordination shell between 0.9 and 2.2 Å as the electronic properties mainly depend on the nearest neighbours. Table 1 summarizes the best fit results for both 40 K and room temperature spectra. The main difference between both temperatures concerns the Debye–Waller (σ^2) factors, higher for the fits at room temperature as expected. Overall, the goodness of the fits is good and confirms a regular FeO_6 octahedral coordination for all samples. This is true even for the Ca-based samples with a monoclinic unit cell. Moreover, the low σ^2 factor at low temperature for this sample is hard to conciliate with phase segregation into two or three monoclinic phases [8, 9] so a spin reorientation seems to be more suitable to account for the phase transition at 150 K developed by this sample [10].

The calculated Fe–O distances are in agreement with the reported crystallographic data [6, 10] and show a high resemblance to the related Mo-based series [21]. The highest Fe–O distance corresponds to the Ba_2 sample whereas the lowest one is shown by Sr_2. Bearing in mind the tabulated effective ionic radii [36], FeO distances close to 2.02 and 2.16 Å are expected for Fe^{3+} and Fe^{2+}, respectively (taking 1.38 Å as the radius for O^{2-}).[2] These values are confirmed by the experimental findings in the reference compounds, i.e. Fe–O values of

[2] The tabulated ionic radius for O^{2-} depends on the coordination number (CN), being 1.35, 1.38 and 1.40 for CN = 2, 4 and 6, respectively. As the CN for oxygen in a perovskite cell can be considered 2 + 4, the value of CN = 4 seems to be the best compromise.

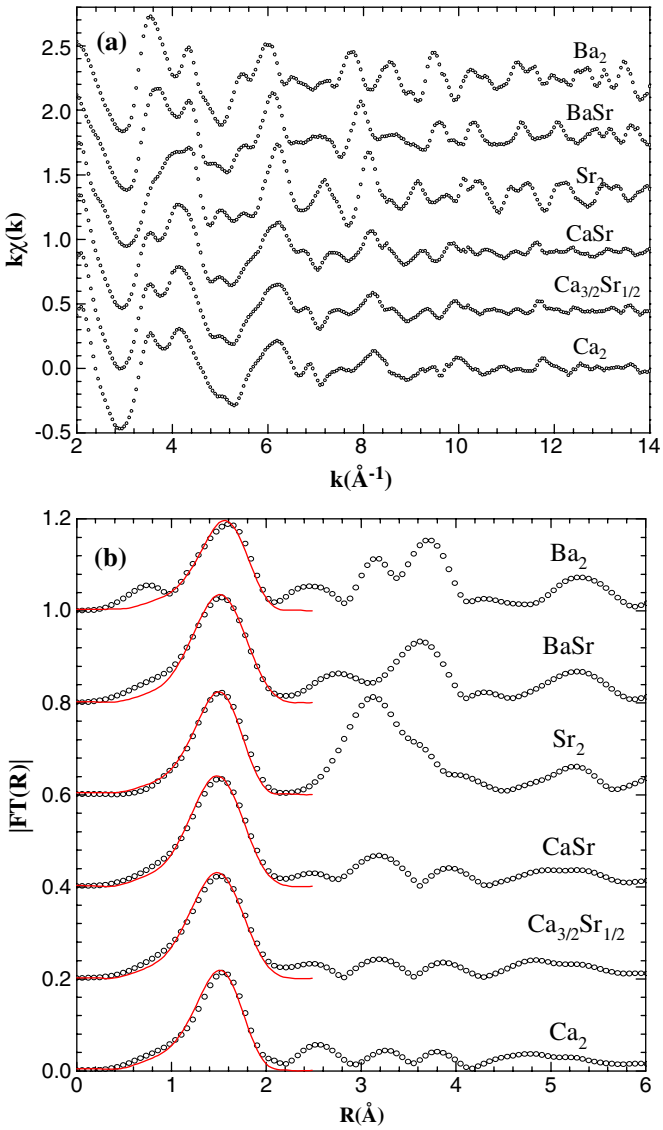

Figure 5. (a) EXAFS spectra, $k\chi(k)$, at the Fe K-edge for A_2FeReO_6 compounds. A_2 is given for each curve and the data were collected at 40 K. (b) Their Fourier transforms that were extracted using a Gaussian window between 2.5 and 13.0 $Å^{-1}$. Solid lines are the best-fit simulations only considering the first-shell oxygen contribution. The spectra are shifted upwards for the sake of clarity.

2.165 and 2.01 Å for FeO [37] and $LaFeO_3$ [38], respectively. Therefore, the data from table 1 are in accordance with the existence of Fe^{3+} in the A_2FeReO_6 series. Only the Ba_2 sample, with higher Fe–O distances, would be consistent with a partial reduction of Fe ions.

Figure 6 displays the EXAFS spectra at the Re L_3-edge for the whole series. Also at this edge, the oscillations are still visible at $k \sim 14$ $Å^{-1}$ and their amplitudes can be correlated to the crystal symmetry, the cubic or nearly cubic samples having the strongest oscillations. Figure 6 also shows the FT of the k-weighted EXAFS spectra between 3.3 and 14.0 $Å^{-1}$

Table 1. Average interatomic distances R [Fe(Re)–O], Debye–Waller factors (σ^2) and reliability factors (R) for the A_2FeReO_6 samples. The R-factor is defined as in [24]. E_0 was fixed to −9.5 and 7.0 eV for Fe K- and Re L_3-edges, respectively. These values are obtained from the fits of the respective references, $LaFeO_3$ and ReO_3. The coordination number has been fixed to six for both edges and s_0^2 was fixed to 0.8 for all fits. Numbers in parenthesis refer to standard deviations of the last significant digit.

		Fe K-edge			Re L_3-edge		
Sample	T (K)	R_{Fe-O} (Å)	σ^2 (Å^2)	R	R_{Re-O} (Å)	σ^2 (Å^2)	R
	40	2.063(6)	0.003(1)	0.037	1.949(4)	0.003(1)	0.025
Ba_2FeReO_6	295	2.067(8)	0.007(1)	0.056	1.950(7)	0.003(1)	0.067
	40	2.026(5)	0.003(1)	0.018	1.943(6)	0.004(1)	0.054
$BaSrFeReO_6$	295	2.026(6)	0.006(1)	0.025	1.947(7)	0.005(1)	0.067
	40	1.993(4)	0.003(1)	0.018	1.942(4)	0.002(1)	0.022
Sr_2FeReO_6	295	1.995(4)	0.005(1)	0.019	1.941(5)	0.003(1)	0.024
	40	2.003(5)	0.002(1)	0.017	1.949(4)	0.002(1)	0.018
$CaSrFeReO_6$	295	2.004(5)	0.004(1)	0.016	1.947(4)	0.002(1)	0.024
	40	2.007(5)	0.003(1)	0.018	1.950(4)	0.001(1)	0.018
$Ca_{3/2}Sr_{1/2}FeReO_6$	295	2.006(5)	0.005(1)	0.015	1.950(4)	0.002(1)	0.020
	40	2.010(5)	0.002(1)	0.031	1.951(3)	0.001(1)	0.017
Ca_2FeReO_6	295	2.012(5)	0.005(1)	0.035	1.951(4)	0.002(1)	0.020

using a Gaussian window. As occurred at the Fe K-edge, the strongest features correspond to the first and second coordination shells. All of the samples have a similar peak at ∼1.5 Å corresponding to the Re–O contribution. The strongest variation among samples is observed in the second coordination shell. The Ba_2 samples exhibit a strong peak that could be ascribed to the narrow distribution of Re–Ba distances in this cubic cell. The opposite is observed for the monoclinic samples with a broad distribution of such distances. Again, these results resemble to those obtained in the homologous Mo series [21].

The structural analysis at this edge is also collected in table 1. The first shell contribution was extracted by Fourier filtering of the FT spectra between 1.0 and 2.2 Å. The best-fit results show a regular ReO_6 octahedron whose average Re–O distance remains nearly invariant for the whole series. Our results are in accordance with crystallographic studies [10]. The Re–O distance of ∼1.95 Å is in agreement with the expected value from tabulated data [36] for Re^{5+} (∼1.96 Å) and significantly higher than the experimental Re^{6+}–O distance (∼1.88 Å) of the reference ReO_3 [28, 39]. Finally, there are no noticeable changes between 40 K and room temperature and even the σ^2 factors remain almost constant in the whole temperature range. In this way, the temperature affects the FeO_6 octahedron more strongly than the ReO_6 one.

4. Discussion and conclusions

This spectroscopic survey allows us to gain insight into the electronic properties of ferrimagnetic double perovskites. Considering the Fe K-edge spectra, both XANES and EXAFS are in agreement with the existence of trivalent iron ions for most of the samples in the A_2FeReO_6 series. The exceptions would be Ba_2 and BaSr samples. According to the chemical shift of the XANES spectra, an oxidation state of +2.75 can be inferred for the former sample and closer to +3 for the latter. According to Fe–O distances calculated from EXAFS spectra, the formal valence for the Ba_2 sample would be +2.7, that nicely agrees with XANES spectroscopy, making our analysis self-consistent. The values deduced for the BaSr sample would lie between the ones calculated for Ba_2 and the rest of the series, i.e. closer to +3. In

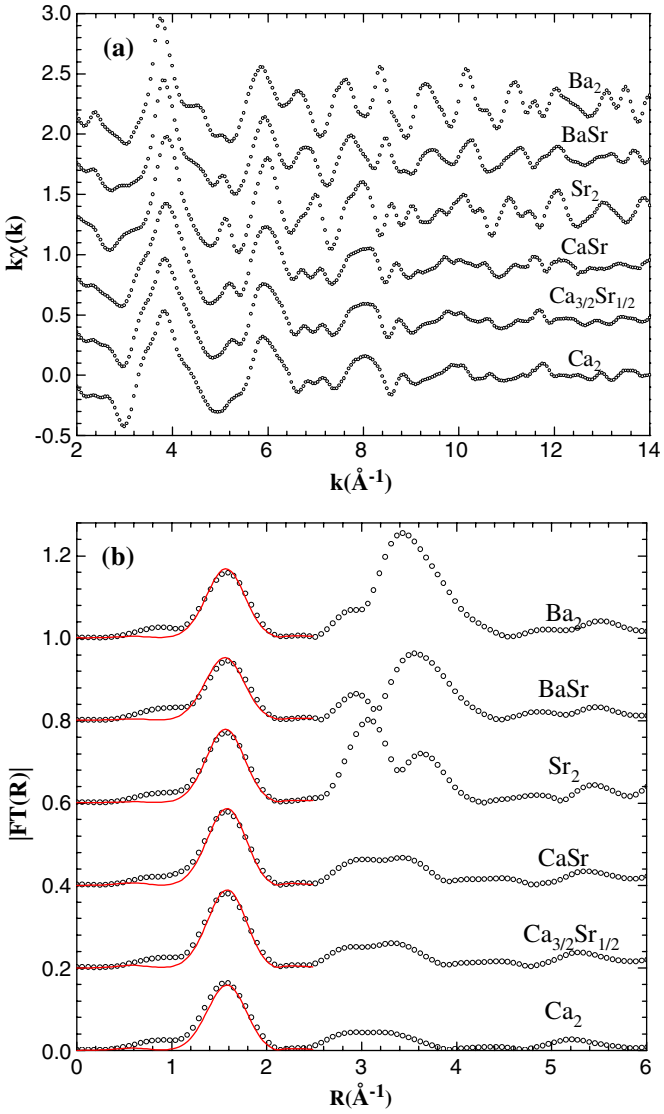

Figure 6. (a) EXAFS spectra, $k\chi(k)$, at the Re L_3-edge for A_2FeReO_6 samples. A_2 is given for each curve. The data were collected at 40 K. (b) Their Fourier transforms extracted using a Gaussian window between 3.3 and 14.0 $Å^{-1}$. Solid lines are the best-fit simulations only considering the first-shell oxygen contribution. The spectra are shifted upwards for the sake of clarity.

any case, it is clear that the presence of Ba strongly affects the oxidation state of Fe atoms in the double-perovskite structure as occurred in Mo-based compounds [21].

Concerning to the Re L-edge spectra, it is worth pointing out the good agreement found in the results obtained from both Fe and Re edges. In this way, the L_1-edge position indicates an oxidation state close to Re^{+5} for all A_2FeReO_6 samples. The L_3-EXAFS has shown a very regular ReO_6 octahedron with small Debye–Waller factors for the whole series that is consistent with the presence of Re^{+5} for all samples including the Ba-based compounds. Therefore, the comparison between EXAFS and XANES seems to point to pentavalent Re for all compounds.

Remembering the assignation of $Fe^{+2.75}$ in the Ba_2 sample, it is clear that a simple ionic model fails to describe this compound. We think this fact could be related to the polarizing power of A^{2+} cations. The bigger the A^{2+} size is, the lower the electron affinity. Therefore, the big Ba^{2+} cation could favour an increase of electron density on the Re–O–Fe sublattice that in this case mainly lies on the Fe atoms.

We notice that the positions of the L_3- and L_2-edges are not very sensitive to Re valence, the chemical shift being rather small. The resonance shapes and intensities instead significantly change for compounds with different nominal valence. All A_2FeReO_6 show a similar double peak in both edges, L_2 and L_3. Such a feature is not observed in the reference compounds (+4 or +6), suggesting an intermediate valence +5 for A_2FeReO_6 samples. The energy splitting is usually ascribed to crystal field and spin-orbit couplings [33, 34] though the presence of two electronic states cannot be discarded. Recent spectroscopic studies have determined the presence of two distinguishable electronic states for Mo ions in Mo-based double perovskites [20]. This is likely to occur in our Ba-based samples, with broad features in some absorption edges, and it would be a suitable explanation for the energy splitting observed in the Re L_3 and L_2-edge XANES spectra (figure 4). However, similar splitting is noticed for all samples, including some without significant mixed valence. Therefore, if there were two electronic states for Re atoms in these double perovskites, they would have similar valence state. Nevertheless, a PES survey on the Re-based double perovskites would be desirable in order to shed light on this subject.

In our measurements, we have not found any signature of the electronic transition developed by Ca_2 and $Ca_{2/3}Sr_{1/2}$ samples at ∼150 K. This seems to point to tiny electronic and geometrical changes such as the spin reorientation proposed in [10]. However, the pre-peak features observed at the L_1-edge (figure 2) that are ascribed to the O 2p–Re 5d mixing can be used as an indicator of the electrical behaviour. Metallic samples show stronger P_L-resonance whereas it is very smoothed for insulating ones.

In our previous study on the related A_2FeMoO_6 series [21], it was very hard to differentiate between Mo^{5+} and Mo^{6+} making use of the Mo K-edge spectra. We concluded in accordance with Szotek *et al* [22] that the ground state may be composed by localized Fe^{3+}/Mo^{6+} and an itinerant electron in the conduction band. Depending on the spin projection of the latter, we could have either Fe^{3+}/Mo^{5+} or $Fe^{(3-d)+}/Mo^{(5+d)+}$ couples. The latter was inferred for Ba-based compounds. This model can also be applied to the Re-based series, but in this case the density projection lies on the Re atom. However, the present study adds new relevant information. The Re L_1-edge is more sensitive to the Re oxidation state. Our study supports the same electronic couple, Fe^{3+}/Re^{5+}, for most of the A_2FeMoO_6 samples. The exception is the Ba-based compounds, but even for these samples a Re^{5+} is found. This result puts forward the importance of the A-electron affinity in the electronic properties of the double perovskites. In this way, measurements on the Mo L_1-edge would be desirable to confirm the role of A atoms in the Mo-based series.

In the case of insulator samples such as Ca_2, $Ca_{3/2}Sr_{1/2}$ and CaSr in the A_2FeReO_6 series, the lack of itinerant electron suggest a localization on the Re atom. Then, our results could be explained in the frame of an ionic picture composed by Fe^{3+} and Re^{5+}. However, this scenario seems to be a very rough approximation. For instance, neutron diffraction experiments revealed that the localized ordered moments are far below those expected for a simple ionic model [8, 10, 11]. This result can be understood instead in the frame of recent LSDA calculations [40] that give an Fe(Re) spin moments of ∼3.7(∼−1.0) μ_B instead of the ideal 5(−2) for Fe^{3+} (Re^{5+}). This reduction has been ascribed to a strong pd hybridization and the agreement with some experimental results, 3.6(−0.9) for Ca_2FeReO_6 [10], is excellent. However, our XANES measurements have shown that insulator samples seem to have lower

pd overlapping (see the inset of figure 2). This result could also be understood in the frame of Wu's calculations [40]. This author suggests that the bending of Fe–O–Re bond angles in Ca_2FeReO_6 leads to a reduced Fe–O–Re pdd–π coupling that results in an insulating behaviour. However, the same lattice distortion produces a finite Fe–O–Re pdd–σ coupling that gives rise to an increase of T_C. If this were true, the P_L features in figure 2 would be a hallmark of the Re t_{2g}–O $2p_\pi$–Fe t_{2g} coupling (or pdd–π mixing) related to the metallic conduction.

Summarizing, our XANES and EXAFS spectra are consistent with the presence of Fe^{3+} and Re^{5+} in the A_2FeReO_6 double perovskites. This survey is also in agreement with a strong pd mixing as inferred from the pre-edge structures below the threshold of both Fe K- and Re L_1-edges. Our results support the importance of pd covalence to account for the physical properties of these samples.

Acknowledgments

We acknowledge the financial support from the Spanish CICyT MAT02-01221 project and from DGA. We thank ESRF for granting beam time and BM29 staff for helping us to perform the experiment.

References

[1] Coey J M D 1999 *Adv. Phys.* **48** 167
[2] Kobayashi K L, Kimura T, Sawada H, Terakura K and Tokura Y 1998 *Nature* **395** 677
[3] Kato H, Okuda T, Okimoto Y, Tomioka Y, Takenoya Y, Ohkubo A, Kawasaki M and Tokura Y 2002 *Appl. Phys. Lett.* **81** 328
[4] Alamelu T, Varadaraju U V, Venkatesan M, Douvalis A P and Coey J M D 2002 *J. Appl. Phys.* **91** 8909
[5] Prellier W, Smolyaninova V, Biswas A, Galley C, Greene R L, Ramesha K and Gopalakrishnan J 2000 *J. Phys.: Condens. Matter* **12** 965
[6] De Teresa J M, Serrate D, Blasco J, Ibarra M R and Morellón L 2004 *Phys. Rev.* B **69** 144401
[7] Kato H, Okuda T, Okimoto Y, Tomioka Y, Oikawa K, Kamiyama T and Tokura Y 2002 *Phys. Rev.* B **65** 144404
[8] Westerburg W, Lang O, Ritter C, Felser C, Tremel W and Jakob G 2002 *Solid State Commun.* **122** 201
[9] Granado E, Huang Q, Lynn J W, Gopalakrishnan J, Greene R L and Ramesha K 2002 *Phys. Rev.* B **66** 064409
[10] Oikawa K, Kamiyama T, Kato H and Tokura Y 2003 *J. Phys. Soc. Japan* **72** 1411
[11] Ritter C, Ibarra M R, Morellón L, Blasco J, García J and De Teresa J M 2000 *J. Phys.: Condens. Matter* **12** 8295
[12] Galasso F S, Douglas F C and Kasper R J 1966 *J. Chem. Phys.* **44** 1672
[13] Sarma D D, Sampathkumaran E V, Ray S, Nagorajan R, Majumdar S, Kumar A, Nalini F and Guru Row T N 2000 *Solid State Commun.* **114** 465
[14] Balcells Ll, Navarro J, Bibes M, Roig A, Martínez B and Fontcuberta J 2001 *Appl. Phys. Lett.* **78** 781
[15] Ray S, Kumar A, Sarma D D, Cimino R, Turchini S, Zennaro S and Zema N 2001 *Phys. Rev. Lett.* **87** 097204
[16] Besse M, Cros V, Barthelemy A, Jaffres H, Vogel J, Petroff F, Mirone A, Tagliaferri A, Bencok P, Decorse P, Berthet P, Szotek Z, Temmerman W M, Dhesi S S, Brookes N B, Rogalev A and Fert A 2002 *Europhys. Lett.* **60** 608
[17] Moreno M S, Goyane J E, Abbate M, Caneiro A, Niebiekikwiat D, Sánchez R D, de Siervo A, Landers R and Zampieri G 2001 *Solid State Commun.* **120** 161
[18] Karppinen M, Yammauchi H, Yasukawa Y, Linden J, Chan T S, Liu R S and Chen J M 2003 *Chem. Mater.* **15** 4118
[19] Zeng Z, Fawcett I D, Greenblatt M and Croft M 2001 *Mater. Res. Bull.* **36** 705
[20] Navarro J, Fontcuberta J, Izquierdo M, Avila J and Asensio M C 2004 *Phys. Rev.* B **70** 054423
[21] Herrero-Martín J, García J, Subías G, Blasco J and Sánchez M C 2004 *J. Phys.: Condens. Matter* **16** 6877
[22] Szotek Z, Temmerman W M, Svane A, Petit L and Winter H 2003 *Phys. Rev.* B **68** 104411
[23] Filipponi A, Borowski M, Bowron D T, Ansell S, DiCicco A, de Panfilis S and Itiè J P 2000 *Rev. Sci. Instrum.* **71** 2422
[24] Rehr J J and Albers R C 2000 *Rev. Mod. Phys.* **72** 621 available at http://FEFF.phys.washington.edu/
[25] Benfatto M, Solera J A, García J and Chaboy J 2002 *Chem. Phys.* **282** 441

[26] García J, Sánchez M C, Subías G and Blasco J 2001 *J. Phys.: Condens. Matter* **13** 3229
[27] Fröba M, Lochte K and Metz W 1995 *J. Phys. Chem. Solids* **57** 635
[28] Kuzmin A, Purans J, Dalba G, Fornasini P and Rocca F 1996 *J. Phys.: Condens. Matter* **8** 9083
[29] Popov G, Greenblatt M and Croft M 2003 *Phys. Rev.* B **67** 024406
[30] Choy J H, Kim D K, Hwang S H, Demazeau G and Jung D Y 1995 *J. Am. Chem. Soc.* **117** 8557
[31] Bare S R, Mitchell G E, Maj J J, Vrieland G E and Gland J L 1993 *J. Phys. Chem.* **97** 6048
[32] Zeng Z, Fawcet I D, Greenblatt M and Croft M 2001 *Mater. Res. Bull.* **36** 705
[33] Groot F M F 1995 *Physica* B **208/209** 15
[34] Choy J H, Kim D K and Kim J Y 1998 *Solid State Ion.* **108** 159
[35] Lede E J, Requejo F G, Pawelec B and Fierro J L G 2002 *J. Phys. Chem.* B **106** 7824
[36] Shannon R D 1976 *Acta Crystallogr.* A **32** 751
[37] Fjellvag H, Gronvold F, Stolen S and Hauback B C 1996 *J. Solid State Chem.* **124** 52
[38] Marezio M and Dernier P D 1971 *Mater. Res. Bull.* **6** 23
[39] Schirber J E, Morosin B, Alkire R W, Larson A C and Vergamini P J 1984 *Phys. Rev.* B **29** 4150
[40] Wu H 2001 *Phys. Rev.* B **64** 125126